

Analytical Solutions to a Problem of Sink-source Flow in a Porous Medium

A. R. Kacimov and Yu. V. Obnosov

*Institute of Mathematics and Mechanics, Kazan State University,
17, University Str., 420008, Kazan, Tatarstan, Russia*

ABSTRACT. New analytical solution to the problem of fluid flow in a porous reservoir composed by rectangular blocks is presented. The Muskat linear, five-point, and chess-type patterns of injection-extraction wells (IEW) are obtained as special cases of this solution. Streamlines, isochrones, breakthrough curves are evaluated in terms of the model of pure advection. Effective conductivity of these patterns is obtained explicitly and compared with Muskat's values which occurred to be good approximations of the rigorous formulae. Numerical procedure of particle tracking is verified on the Rankine flow pattern for a pair of IEW placed in an uniform groundwater flow and the Polubarinova-Kochina solution for a pumping well in an aquifer with a circular inhomogeneity. Applications to a network of octogonal honey-comb blocks and filled fractures-orifices are discussed.

Mathematical modeling of fluid flow and chemical transport in subsurface under influence of IEW systems is of great importance both in petroleum engineering and hydrology. These systems are used in flooding technique (Muskat 1946), in drainage (Strack 1989), in pump-and-treat methods for remediation of contaminated aquifer zones (USEPA 1992). In the classical approach IEW are simulated as sources and sinks, and a porous reservoir/aquifer is assumed homogeneous. This allows for analytical description for pressure (hydraulic head), velocity, particle travel times, *etc.* (Muskat 1946, Polubarinova-Kochina 1977). These characteristics describe the advective component of contaminant transport (Anderson and Woessner 1992). However, any real reservoir or aquifer is heterogeneous and only few analytical

solutions are known even for simplest models (one-phase fluid, confined aquifer, step-wise constant change of conductivity, *etc.*). Novel mathematical approach developed by Emets and Obnosov (1989, 1990), Obnosov (1992) allows for explicit description of advection with rigorous refraction conditions along the boundaries between media of different conductivity. Recently, this approach was used in applications to ground water flows in aquifers (Kacimov and Obnosov 1994, 1995).

In this paper we present explicit rigorous description of the problem of flow in a reservoir containing double-periodic lens-type rectangular inclusions. As a result, the imposed natural flow becomes 2-D with curved streamlines and contaminant transport follows 'fingered' or 'channeled' flow paths. We use the simplest model of pure advection and neglect all other mechanisms (block sorption, microdispersion, *etc.*).

First, we investigate the limiting case when blocks are impermeable. The corresponding solution describes the velocity (specific discharge) field as an anti-holomorphic function within an elementary cell (rectangle) with sink-source singularities at its vertexes. As special cases we obtain the well-known IEW systems exhibiting symmetry. Thus, the linear pattern (LP), the chess-type pattern (CTP), in particular, the five-point pattern follow from the general case at equal rates of injection-pumping. Our solutions are presented in closed form in terms of elliptic functions and supplement the Muskat series expansions. As a check on the particle tracking procedure used we calculate streamlines, isochrones, and averaged velocities for two common hydrological schemes. Namely, we consider a dipole (IEW pair) in a uniform ground water flow as a Rankine body. This scheme is used both in tracer experiments and pump-and-treat systems for aquifer remediation. Then we use the Polubarinova-Kochina analytical solution to compute the advective characteristics mentioned for a pumping well in an aquifer containing a circular inhomogeneity. At last we discuss applications of the lens system to networks modeling a fractured medium with octogonal blocks.

Reservoir with lens-type inclusions

Consider a porous reservoir composed by two porous media, highly permeable conduits with conductivity k_1 and low permeable blocks with conductivity k_2 . The two phases repeat themselves in a double-periodic manner as a checkerboard structure (Fig. 1a) such that geometrical sizes of rectangular blocks and conduits are l and h . The natural flux vector through one rectangle of the system, J , is oriented arbitrary relative to the rectangles; a and b are the horizontal and vertical components of J :

$$\int_0^h \Re V_1(iy) dy = a, \quad \int_0^l \Im V_1(x) dx = b.$$

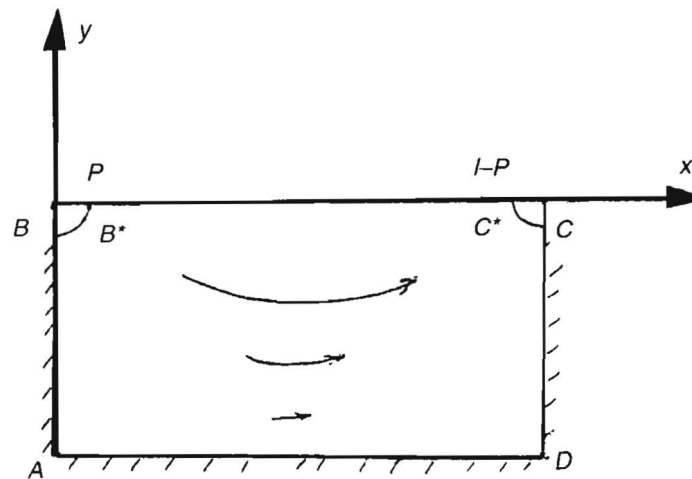


Fig. 1 a) the checkerboard medium,

$$k[m, r] := 1 / (2/Pi \text{ Log} [(Jacobi DN[2 \text{ EllipticK}[m] r, m] + Jacobi CN[2 \text{ EllipticK}[m] r, m]) / (Jacobi DN[2 \text{ EllipticK}[m] r, m] - Jacobi CN[2 \text{ EllipticK}[m] r, m])])$$

$$u2 = \text{Plot3D}\{k[m, r], \{m, 0.01, 0.99\}, \{r, 0.01, 0.1\}\}$$

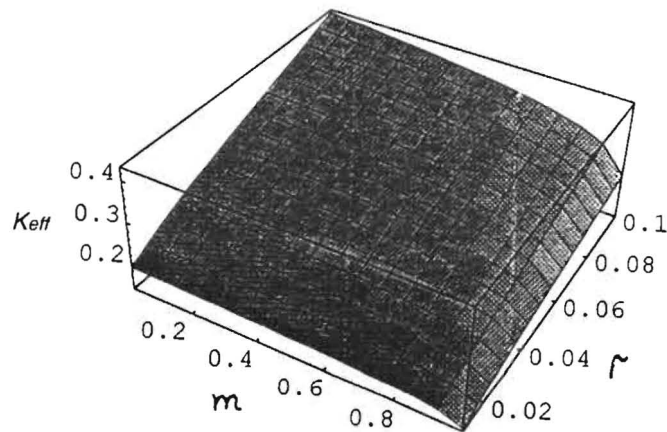


Fig. 1 b) the lensed medium,

```

kmuskat (r_, m_) := 1/ (2 Pi Log [
Sinh [Pi EllipticK[m] / EllipticK[1-m] ]^4*
Sinh [3 Pi EllipticK[m] / EllipticK[1-m] ] /
Sinh [Pi r EllipticK[m] / EllipticK[1-m] ]^2/
Sinh [2 Pi EllipticK[m] / EllipticK[1-m] ]^3)
u1 = Plot3D[kmuskat[r,m], {m, 0.01, 0.99}, {r, 0.01, 0.1}]

```

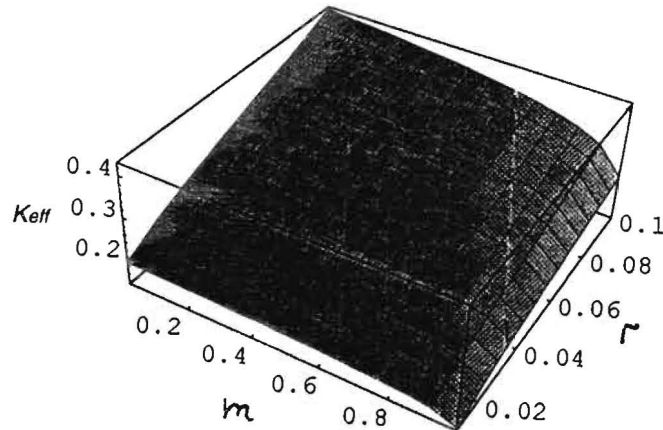


Fig. 1 c) flow near two adjacent corners of impermeable lenses.

where V_1 is the specific discharge vector within $ABCD$ and \Re and \Im designate the real and imaginary parts of a complex function.

Note, that the medium in Fig. 1a is a limiting case of the medium with arbitrary distances H , L between blocks (Fig. 1b) when $H \rightarrow h$, $L \rightarrow l$ (the checkerboard structure is shown in Fig. 1b by dashed lines). These types of lensed structures are of interest in studies of highly tortuous flow paths through porous units with repeating inhomogeneities (Firoozabadi and Markeset 1995, Kinzelbach 1992, Kung 1990).

Obnosov (1996) derived a rigorous solution to the flow problem shown in Fig. 1a with arbitrary k_1/k_2 . Unfortunately, the general case with arbitrary L and H in Fig. 1b proved to be difficult for explicit description. In what follows we shall study in details one special case of the medium in Fig. 1a when block conductivity $k_2 = 0$.

We assume fully saturated Darcian steady seepage of incompressible one-phase fluid in an isotropic incompressible porous medium such that transmissivity varies in a chess-like type because of step-wise changes of conductivity. Introduce the complex coordinate $z = x + iy$ and the complex potential $\omega_{1,2} = \phi_{1,2} + i\psi_{1,2}$, where $\phi_{1,2}$

is the velocity potential and $\psi_{1,2}$ is the stream function which are harmonic within conduits (1) and blocks (2). The specific discharge vector, $V_{1,2} = \overline{d\omega_{1,2}/dz}$, is an antiholomorphic function within these rectangles (overlining means complex conjugation). Along the rectangle boundary the known refraction conditions hold:

$$\phi_1/k_1 = \phi_2/k_2, \quad \psi_1 = \psi_2$$

that can be equivalently reformulated as continuity of the normal and prescribed ratio of tangential discharge components (Polubarinova-Kochina 1977).

In the Obnosov's (1996) general solution for the two-component cell ABA_2D_2CD we set $k_2 \rightarrow 0$. Then the velocity V within the only conductive cell $ABCD$ is

$$\overline{V(z)} = \frac{c_1}{\text{sn}(Z|m)} + i \frac{c_2}{\text{sn}(iZ|m_1)} \quad (2.1)$$

where $Z = 2Kz/l$ and two real constants c_1, c_2 will be defined below. $K(m)$ designates the complete elliptic integral of the first kind. Its parameter m is easily derived from the equation:

$$K/K' = l/h$$

where $K' = K(m_1)$, $m_1 = 1 - m$.

Here and below sn , dn , cn , ds , cs designate Jacobian elliptic functions (Abramovitz and Stegun 1970). Subindex '1' for these functions will denote in what follows the same functions with parameter m_1 .

Near the vertexes solution (2.1) exhibits sink-source singularities. The strength of these singularities are calculated as mathematical residues of $V(z)$ (since we treat now only one porous component we omit subindexes indicating the media):

$$q_A = -q_C = (c_1 - c_2) \frac{l}{2K}, \quad q_B = -q_D = (c_1 + c_2) \frac{l}{2K} \quad (2.2)$$

Thus, locally, near the vertexes the flow behaves like in vicinity of a quadrant of IEW with radial diverging-converging streamlines. Obviously, (Muskat 1946) the rate of these wells is expressed as

$$q_{A,B} = \frac{\pi}{2} \text{res}_{A,B} \overline{V(z)}$$

Where res designates the residue value that is easily calculated from (2.1). How to relate now the vector of imposed flux J with q_A and q_B ? The corresponding procedure is very simple. We present J as a vector sum of two orthogonal components J_A and J_B which are oriented at angle $\pi/4$ with respect to the coordinate axis (recall that singularities at vertexes provide just this orientation of J_A and J_B). Then, $q_A = J_A$, $q_B = J_B$.

Sinks and sources in (2.1) approximate the circled zones in Fig. 1b when these zones are narrow as compared to l and h . At the corner points a detailed flow pattern (Fig. 1c) can be evaluated by the method of conformal mappings (for brevity we omit the corresponding derivations). Noteworthy, that for two neighbour conductive cells, say $ABCD$ and $AB_1C_1D_1$, if the joint point A is a sink for $ABCD$ then it is a source of the same intensity for $AB_1C_1D_1$ and *vice versa*.

To get the advection characteristics we express the real u and imaginary v parts in (2.1) (Abramovits and Stegun 1970). Since we deal now only with one rectangle we go to the coordinate system originating at the center of $ABCD$ and use a well-known particle-tracking method (Anderson and Woessner 1992) with a routine fourth-order Runge-Kutta integration of system:

$$dx/dt = u(x,y)/v, \quad dy/dt = v(x,y)/v,$$

$$u = \sqrt{m} (c_1 A \text{cn}X \text{dn}X \text{dn}_1 Y - c_2 \sqrt{mm_1} B \text{sn}X \text{cn}X \text{sn}_1 Y),$$

$$v = \sqrt{m_1} (c_1 \sqrt{mm_1} A \text{sn}X \text{sn}_1 Y \text{cn}_1 Y - c_2 B \text{dn}X \text{cn}_1 Y \text{dn}_1 Y)$$

$$A = \frac{\text{cn}^2 X + m_1 \text{sn}^2 X \text{sn}_1^2 Y}{\text{cn}^2 X \text{dn}^2 X \text{dn}_1^2 Y + m_1^2 \text{sn}^2 X \text{sn}_1^2 Y \text{cn}_1^2 Y} \quad (2.3)$$

$$B = \frac{\text{cn}_1^2 Y + m^2 \text{sn}^2 X \text{sn}_1^2 Y}{\text{dn}^2 X \text{cn}_1^2 Y \text{dn}_1^2 Y + m^2 \text{sn}^2 X \text{cn}^2 X \text{sn}_1^2 Y}$$

where $X = 2Kx/l$, $Y = 2Ky/l$, x , y are marked particle coordinates, v is porosity of the conduit.

We started with two sets of points which consist of M particles placed at $t = 0$ along the quarter-circles surrounding points A and B : $z_j = \mp ih + \rho \exp [\pm i j \pi / (2M)]$,

$j = 1, 2, \dots, M$ where ρ is a small value (well radius in Muskat's solution) and the \pm signs correspond to points A and B , respectively. This choice is made to connect our results with Muskat's one though initial position of tracked particles can be arbitrary.

Fig. 2 shows in coordinates $x - l/2, y - h/2$ eight streamlines ($M = 4$) for $q_B/q_A = 0.5$, $\rho/l = 0.01$ for three ratios $l/h = 0.82, 0.67, 0.53$ (graphs a-c, respectively). Obviously, within a cell two points (E_1, E_2) of zero velocity exist that are placed on the sides of the rectangle that connect two sinks and two sources. Two separatrices shown schematically by dashed lines in Fig. 1a split the flow into three parts.

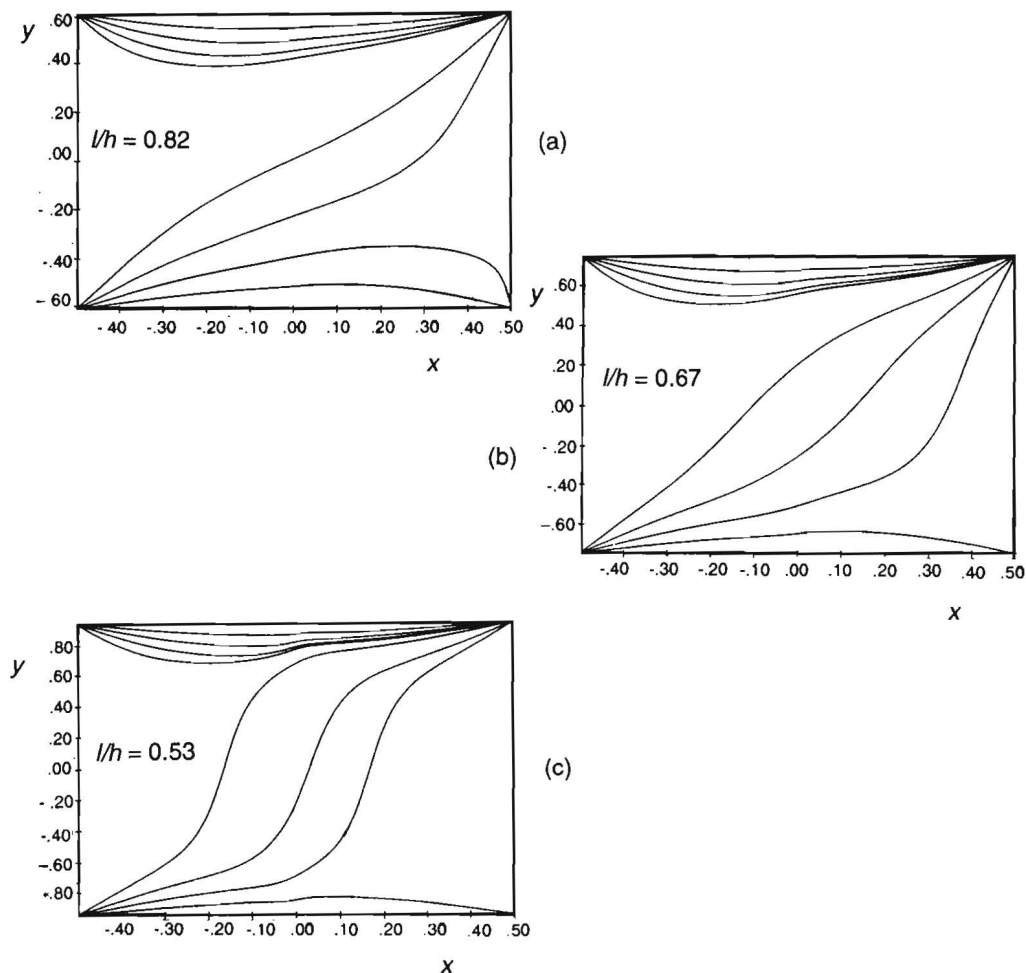


Fig. 2. Streamlines for three l/h ratios and $q_B/q_A = 0.5$.

An important characteristic of solute transport in subsurface is the breakthrough curve which in terms of our model (piston-like displacement) follows from $T(\theta)$ distribution where θ is the angular coordinate of starting points. The total time T which is needed for a particle (marked by θ) to pass the cell was calculated as a sum of time steps in the Runge-Kutta procedure. The graphs for T as functions of $(2\theta/\pi)$ for the particles started from the vicinity of the point A ($l/h = 0.78$, $\nu = 0.2$, $\rho/l = 0.01$) are shown in Fig. 3; curves 1-3 for $q_B/q_A = 0.0, 0.5, 1.0$, respectively. For the general case with arbitrary q_B/q_A calculations show two peaks on these graphs ($T = \infty$) that correspond to two stagnation points E_1 and E_2 . For example, curve 2 in Fig. 3 exhibits one 'inner' maximum. Note, that this and other extrema shown are finite since we used a discrete set of marked particles. For $q_B = 0$, $T = \infty$ at $\theta = \pi/2$ and $\theta = 0$. For another limiting case $q_A = q_B$ the two peaks coincide and correspond to $\theta = \pi/2$.

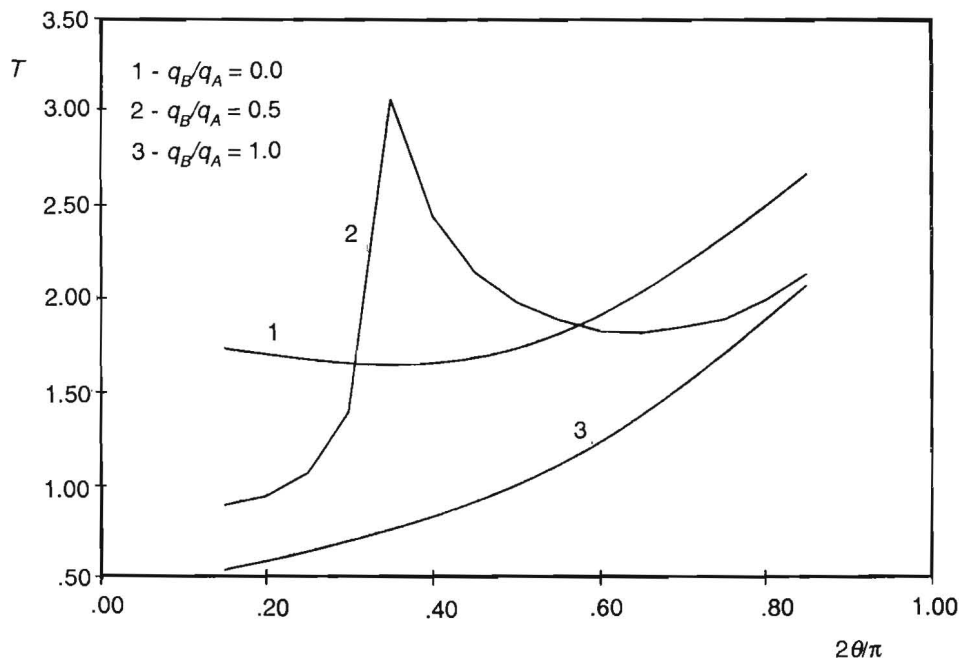


Fig. 3. Travel times for three q_B/q_A ratios and fixed l/h .

Muskat's systems

In the oil extraction industry, various combinations of IEW are used in flooding regimes. The linear pattern and chess-type pattern were analytically described by summation of corresponding source-sink terms in terms of pressure (Muskat 1946).

The corresponding formulae for effective conductivity (resistivity) and efficiency of IEW networks are widely used in petroleum engineering (Petroleum Production Handbook) for preliminary estimations though the Muskat's model assumptions (one-phase Darcian flow, homogeneous reservoir, *etc.*) are very restrictive.

The main questions are: What is the error of Muskat's formulae? Are they valid for arbitrary distance ratio between two neighbouring wells and rows? How simple is the exact result valid uniformly for arbitrary ratio? We shall derive the pressure and velocity for LP and CTP in closed form. In particular, we express rigorously the effective resistivity of the systems.

Setting $q_A = q_B = q$ in (2.2) and, hence $c_2 = 0$, we obtain an element of LP (Fig. 4a). At $q_B = 0$, $q_A = q$ ($c_1 = -c_2$) we go to CTP velocity distribution (Fig. 4b). The last pattern at $l = h$ is reduced to a five-point pattern. Assume as usually that a well is modeled as a circle of small radius ρ and the pressure (head) fall between two neighbouring IEW is $\delta_{p,p} = -\phi/k$. Then effective conductivity of a cell of the patterns under study is defined as $k_{eff} = q/\delta p$.

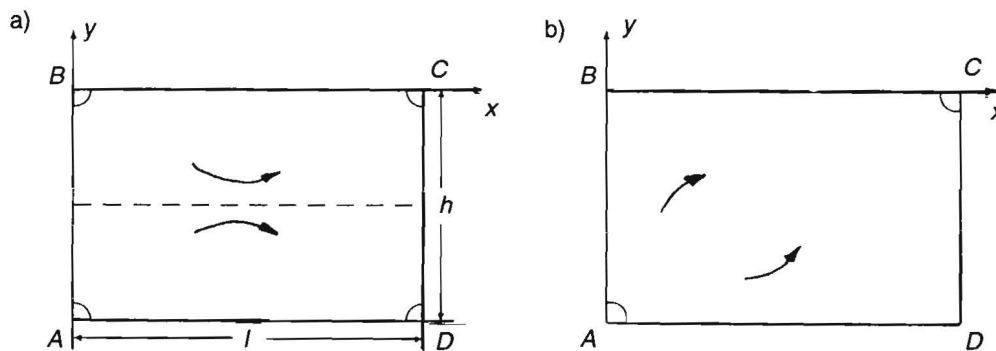


Fig. 4. One element of a) linear pattern of IEW, b) chess-type pattern of IEW.

Let us derive the potential and stream function distributions. For that purpose we integrate (2.1) and obtain the complex potential as follows:

$$\omega = \frac{c_1 l}{2K\sqrt{m}} \ln [ds(Z) - cs(Z)] + \frac{c_2 l}{2K\sqrt{m_1}} \ln [ds_1(iZ) - cs_1(iZ)] \quad (3.1)$$

Expressing the real and imaginary parts in (3.1) we go to $\phi(x,y)$, $\psi(x,y)$ and

hence $\delta p = k[\phi(\rho, 0) - \phi(l - \rho, 0)]$. Then, for LP we derive from (3.1)

$$k_{eff} = \left[\frac{2}{\pi} \ln \frac{dn u + cn u}{dn u - cn u} \right]^{-1} \quad (3.2)$$

where $u = 2K\rho/l$.

Muskat obtained this value in an approximate way for $l/h > 0.24$ in the following form

$$k_{eff} = \left[\frac{2}{\pi} \ln \frac{\sinh^4 f \sinh 3f}{\sinh^2 r \sinh^3 2f} \right]^{-1} \quad (3.3)$$

where $f = \pi l/h$, $r = \pi\rho/h$. Fig. 5 illustrates k_{eff} as function of l/h for $\rho/l = 0.075$ in accordance with (3.3) (curve 1) and (3.2) (curve 2). Comparing curves 1 and 2 we can conclude that Muskat's approximation is very close to rigorous expressions even for small l/h .

For CTP $\delta p = k[2\phi(0, -h + \rho) - \phi(0, 0) - \phi(l, -h)]$ and k_{eff} is derived from (3.1) after some algebra similar to LP as

$$k_{eff} = \frac{\pi}{2} \left[\ln \frac{dn(u/2) dn_1(u/2)}{sn(u/2) sn_1(u/2) \sqrt{mm_1}} \right]^{-1} \quad (3.4)$$

Muskat's k_{eff} for this pattern reads

$$k_{eff} = \left[\frac{2}{\pi} \ln \frac{\cosh^4(f/2) \cosh^3(3f/2)}{\sinh^2(r/2) \sinh^4 f \sinh(2f)} \right]^{-1} \quad (3.5)$$

In (3.4) standard series expansions for $\ln dn x$ and $\ln sn x$ were used.

Fig. 5 presents k_{eff} as function of l/h for CTP at $\rho/l = 0.075$ according to (3.5) and (3.4) (curves 3 and 4, respectively). The graphs again show that Muskat's approximation differs from the rigorous results only at small values of l/h .

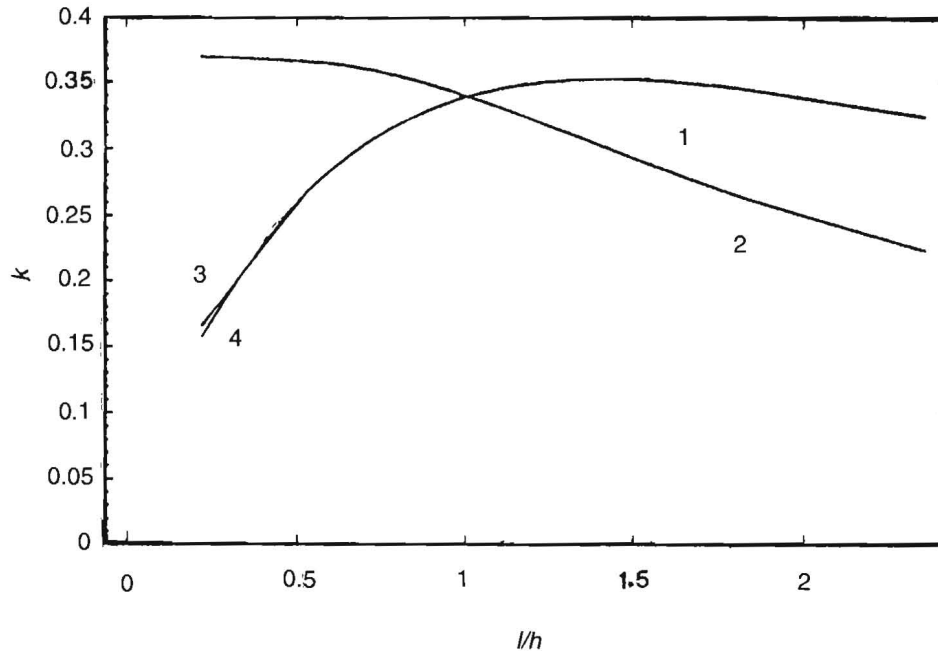


Fig. 5. Rigorous and Muskat's values for effective conductivity of LP and CTP.

Note that in Muskat's book k_{eff} values are four times higher than ours since we consider only quarters of singularities. Thus, to return to whole LP or CTP of wells one should multiply eqns (3.2) and (3.4) by a factor of 4.

Thus, Muskat's approximations are valid for broader l/h ratios of IEW systems than indicated by Muskat himself and can be complemented by rigorous formulae (3.2), (3.4) if necessary.

Hydraulic barriers as Rankine's bodies

To prevent or reduce ground water flow through a certain area of an aquifer, several options are available, such as engineering barriers and hydraulic barriers among others (Child 1985, Philip and Walter 1992, USEPA 1992, Wilson 1984). Engineering barriers include sealing, grouting, lining or other means of isolation of a

contaminated zone (CZ) by modifying the permeability of the porous medium where the flow takes place. Note, that reduction of flow through the zone of potential danger (porous waste repository, areas with adsorbed contaminants caused by leakage *etc.*) may be gained by its shielding with both low and high permeable liners (Kacimov and Obnosov 1994, Rowe 1988). Hydraulic barriers control the flow field by means of hydrodynamical disturbance of the natural flow using recharge-discharge wells or horizontal drains. Along with plume isolation by dividing surfaces (separatrices) these barriers can intensify flushing of CZ (pump-and-treat systems). At times engineering barriers are costly and a hydraulic barrier may be preferable. A simple technique for confining CZ is based on installation of IEW that interfere with the natural flow to produce closed 'internal' circulation areas. If a CZ is isolated within one of these areas, contaminant transport to the 'external' flow will be solely by diffusion. Hence, providing sufficiently intensive circulation by force of pumping-injection rates one may both protect the aquifer and remediate the contaminant zone.

To study a pair of IEW we apply the solution developed by Rankine (1871) for calculation of the effect of different shaped ships on uniform flows of ideal fluid. The Rankine technique allows for explicit presentation of heads, streamlines, velocities for combination of 2-D or 3-D sinks and sources with the natural gradient. The Rankine ideas is commonly employed in aerodynamics where combinations of distributed singularities (sinks, sources, doublets, multipoles) are widely used for evaluation of flow patterns, near airfoils, bodies of revolution, wings, *etc.* However, hydrologists are not well acquainted with the pioneering paper by Rankine though the method is used in practice (Polubarinova-Kochina 1977, Strack 1989).

We utilize two of Rankine's flow schemes to evaluate the hydraulic barrier problems mentioned above. Though the problem of a dipole in an uniform flow is well studied (Grove *et al.* 1970) we repeated calculations of hydraulic characteristics to relate them with Rankine's analytical formulae. Specifically, we compute streamlines and travel times for a source-sink pair placed symmetrically in the natural flow for the 2-D and 3-D cases using velocities calculated from the Rankine explicit solution. Obviously, for ship design purposes, Rankine was not interested in the inner flow area confined by dividing surface and he stated: "In the present investigation, the external streamlines alone will be considered". In contrast, we restrict ourselves to the 'internal' area where two wells interact. In addition we discuss briefly the case of non-steady recharge-discharge rates.

Consider the natural flow with velocity J (m/sec) in a confined aquifer of constant conductivity where CZ to be isolated is located. The Laplace equation holds

for the velocity potential ϕ . The Stokes' stream function Ψ satisfies the equation:

$$\frac{\partial^2 \Psi}{\partial x^2} + \frac{\partial^2 \Psi}{\partial y^2} - \frac{\partial \Psi}{x \partial x} = 0$$

where x and y in 3-D case are coordinates in a plane passing through the two singularities.

Place a 3-D source W_1 and a 3-D sink W_2 of equal strength $Q(m_3/sec)$ along the line that coincides with the direction J and the Ox axis such that the distance between the two singularities is $2a$. An interface separates the flow in to 'internal' and 'external' parts and is symmetric about the Ox axis. Fig. 6 presents the upper half of plane through the Ox axis. Assume that the aquifer thickness is large enough to ignore the influence of its top and bottom on the source-sink interaction such that the source and sink model an injection well and a pumping well, respectively, whose screen lengths are comparatively small.

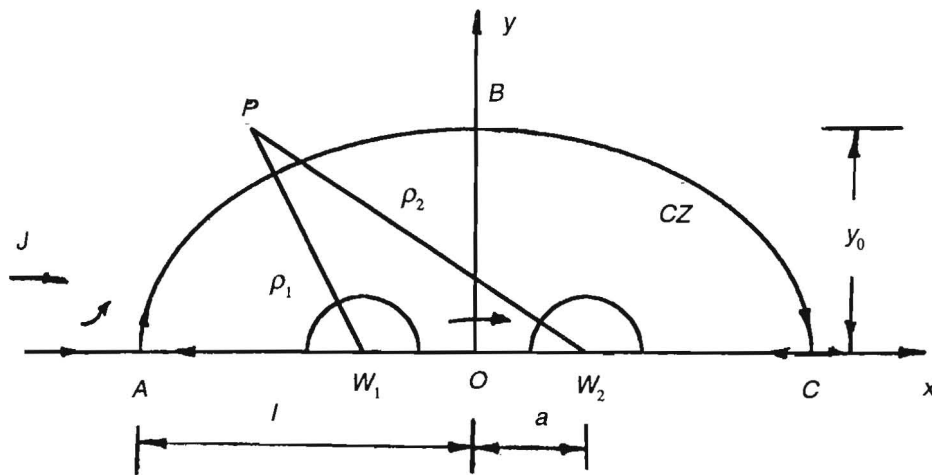


Fig. 6. One half of the Ranker body.

According to Rankine, the velocity potential and stream function are given by:

$$\phi = Jx + \frac{q}{4\pi} [1/\rho_1 - 1/\rho_2], \quad (4.1)$$

$$\Psi = \frac{Jy^2}{2} + \frac{Q}{4\pi} \left[\frac{x-a}{R_1^{1/2}} - \frac{x+a}{R_1^{1/2}} \right] \quad (4.2)$$

Where $R_1 = (x - a)^2 + y^2$, $R_2 = (x + a)^2 + y^2$, and ρ_1, ρ_2 are distances from arbitrary point P in the flow region to the source and sink, respectively. Specific discharge components, $u = \partial\phi/\partial x = y^{-1} \partial\Psi/\partial y$, $v = \partial\phi/\partial y = -y^{-1} \partial\Psi/\partial x$, at all points inside the flow interface (barrier) are obtained from (4.1), (4.2) as:

$$u = J + \frac{Q}{4\pi} \left[\frac{x+a}{R_2^{3/2}} - \frac{x-a}{R_1^{3/2}} \right], \quad v = \frac{Qy}{4\pi} \left[\frac{1}{R_2^{3/2}} - \frac{1}{R_1^{3/2}} \right] \quad (4.3)$$

We start particle tracking according to (4.3) from the injection site initial points $x_0 = -a + \rho \cos\theta$, $y_0 = \rho \sin\theta$, $0 \leq \theta \leq \pi$ (ρ is the radius of a small sphere which represents the well) and track a particle until it reaches $x = 0$. Because of symmetry, the part from $x = 0$ to $x = a$ is the same as from $x = 0$ to $x = -a$ and need not be recalculated. The Rankine body of revolution confining the well-circulation area results from rotation about the Ox axis of the dividing streamline ABC, which is obtained by putting $x_0 = -a - \rho$, $y_0 = 0$ i.e. $\theta_0 = \pi$ as initial condition in equation (3). The horizontal, $2l$, and vertical, y_0 , dimensions of the ovoid are derived from the equations:

$$y_0^6 + a^2 y_0^4 - a^2 \alpha^2 = 0, \quad (l^2 - a^2)^2 - a\alpha l = 0$$

where $\alpha = Q/(\pi J)$. The parameters l and y_0 are shown in Fig. 7 in nondimensional form: $y_0 \alpha^{-1/2}$ and $l \alpha^{-1/2}$ as a function of $a \alpha^{-1/2}$ (curves 1 and 3, respectively).

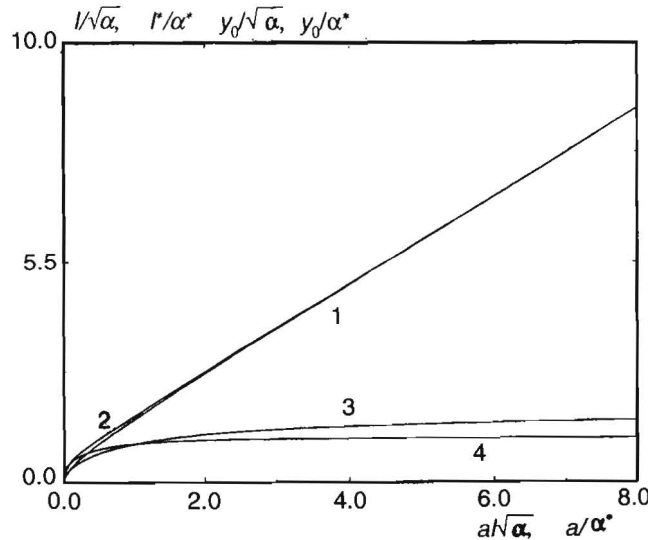


Fig. 7. Horizontal and vertical sizes of circulation zone for 3-D dipole.

Note that A and C are stagnation points and travel time along W_1ABCW_2 is infinite. To estimate dispersion coefficients that are commonly used in the convective dispersion equation, the mean velocity V_m along the streamlines is derived as $V_m(\theta) = S(\theta)/t(\theta)$ where $S(\theta)$ is the length of the streamline (Grove and Beteem 1971). The last value was also calculated during step-by-step integration of equation (3). Fig. 8 shows streamlines for one quadrant of the 'internal' flow area for $Q=1$, $J=1$, $a=1$, $r=0.01$. Curves 1-6 correspond to starting points with $\theta/\pi = 0.95, 0.75, 0.55, 0.35, 0.15,$ and 0.05). Travel times and mean velocities for the same parameters and $\nu=0.3$ are depicted in Fig. 9 (curves 1 and 2, respectively).

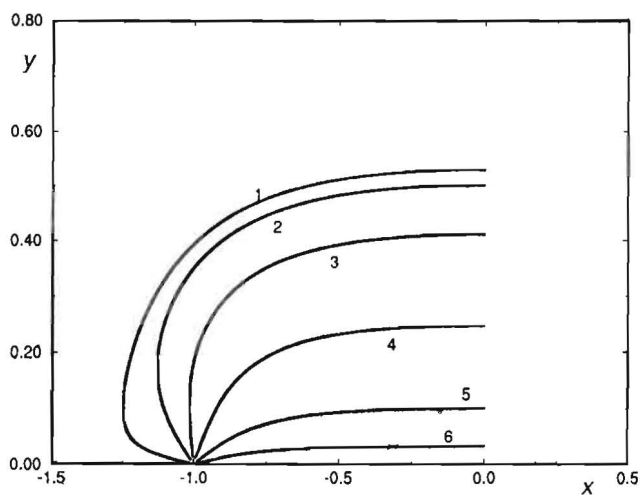


Fig. 8. Streamlines for 3-D dipole.

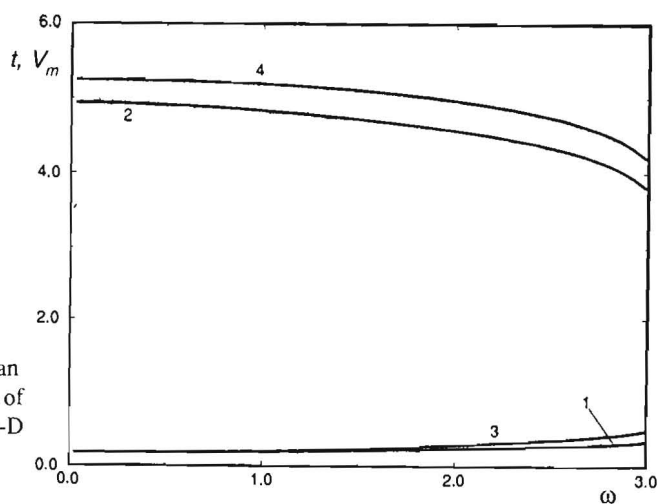


Fig. 9. Travel times and mean velocities as functions of starting point angle for 3-D and 2-D dipoles.

Consider now a 2-D flow pattern when the two wells of rate $Q(m^2/sec)$ per unit aquifer depth being modeled as a source-sink pair (the well screen penetrates the whole depth of the aquifer). In this case the dividing surface is a cylinder which plane section (left half) is again shown in Fig. 6. For the same designations as for the 3-D case above the components of velocity are:

$$u = J + \frac{Q}{2\pi} \left[\frac{x+a}{R_2} - \frac{x-a}{R_1} \right], \quad v = \frac{Qy}{2\pi} \left[\frac{1}{R_2} - \frac{1}{R_1} \right] \quad (4.4)$$

Horizontal size, $2l^*$, and vertical size, y_0^* , of the dividing cylinder are derived as follows

$$(l^*)^2 = a^2 + a\alpha^*, \quad a = y_0^* \tan(y_0^*/\alpha^*), \quad \alpha^* = Q/(\pi J).$$

The values of y_0^*/α^* and l^*/α^* as functions of a/α^* are shown in Fig. 7, curves 2 and 4, respectively. The system of two ordinary differential equations of the particle tracking method with explicit functions (4.4) was intergrated as for the 3-D case. The corresponding quadrant of streamlines is shown in Fig. 10 for $Q = 1$, $J = 1$, $a = 1$, $r = 0.01$. Curves 1-6 correspond the same starting points as for the 3-D case. The corresponding travel times and mean velocities are plotted in Fig. 9 (curves 3 and 4, respectively).

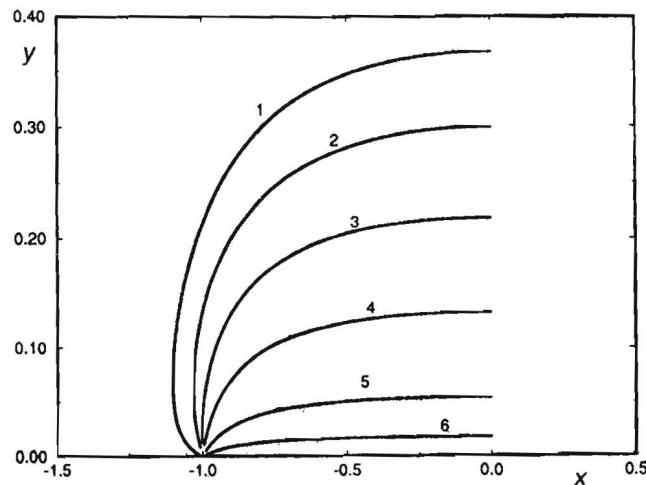


Fig. 10. Streamlines for 2-D dipole.

Note, that travel times along the streamlines passing through CZ may be compared with diffusion times from points within CZ to the boundary ABC. Such empirical comparisons can be used for crude estimations of advection-diffusion relation when modeling contaminant transport.

Rankine's model can be used for systems subjected to transient conditions, for example, pulsed pumping (USEPA 992). This innovative technique involves periodic pumping-injection rates $Q^*(t)$ that allow for activation of flow paths in the stagnation zones. We illustrate the effect of non-steady flow perturbations using the regime $Q^* = Q + q \sin(\omega t)$, where Q is the mean rate, $\omega = 2\pi/T$, T is the period, and q is the amplitude of rate oscillations. For brevity we consider the 2-D case only.

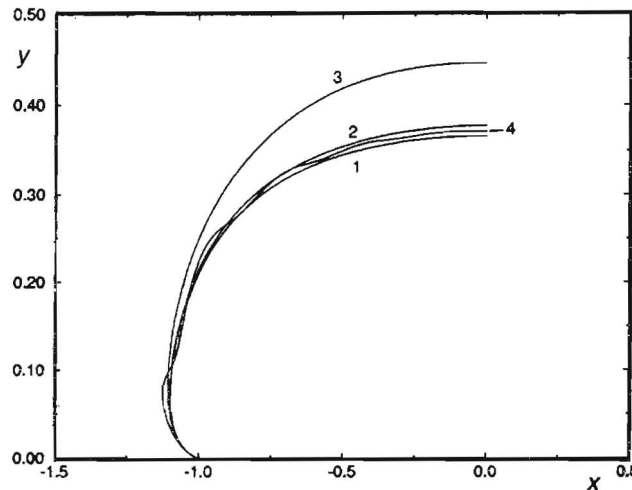


Fig. 11. Streamlines for 2-D transient dipole flows.

Fig. 11 presents a quarter of the 'pulsing' Rankine body with $\theta/\pi = 0.95$ for the same parameters as in Fig. 10, $q = 0.5$ and $\omega = 0.01, 1.0, 10.0,$ and 100.0 (curves 1-4, respectively). From the graphs plotted we see that a particle can deviate from its steady trajectory by injection-pumping fluctuations. Computations showed that the closer a particle to ABC the stronger it deviates from the steady route which is clear from elementary balance quantities. The theory of corresponding systems of ordinary differential equations (non-autonomous in mathematical terms, see, for example, Arnold 1983) is actively studied in applications to mixing regimes in chemical technology, fluid mechanics, *etc.*

Clearly, the transient regime calculated bears all the restrictions of the model implemented. Assumptions about incompressibility and as a consequence the Laplace equation for the potential are restrictive since in reality oscillations of well rates are dissipated both by matrix and liquid that calls for more complex models.

Circular inclusion affecting a pumping well

Some regimes of aquifer remediation involve temporary halt of injection/pumping to/from a well while other wells continue to operate. In this case the stopped well becomes hydrodynamically passive though its screen and changes of near-well zone permeability due to previous usage disturb the ground water flow. Consider the simplest case assuming a pumping well being placed at the point $z = x_0$ and a stopped injection well at the point $z = 0$. The stopped well has a screen of radius R , conductivity k_2 and aquifer conductivity is k_1 , porosities of the two media are v_1 and v_2 . Fig. 12 shows streamlines for this system at $k_2/k_1 = 0.3$. Strictly speaking, the pumping well has its own screen which conductivity differs from k_1 . However, this well is hydrodynamically active and we neglect this conductivity difference substituting the well by a sink in the locally homogenous surrounding. This approximating leads to deviation from the exact value only near $z = x_0$.

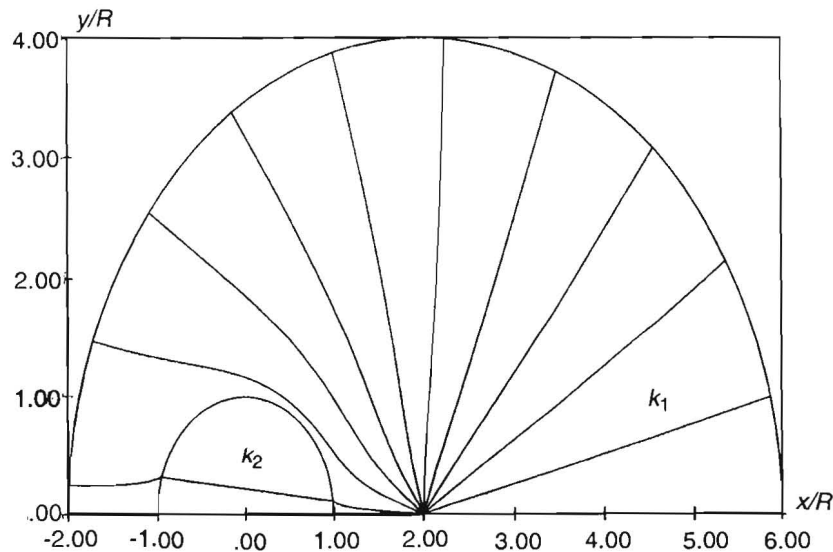


Fig. 12. Flow to a pumping well near a circular inclusion.

The main question is: how strong is the influence of inhomogeneity on the travel time distribution?

The rigorous solution to the flow problem under consideration was obtained many years ago (Polubarinova-Kochina 1977). Here we use this solution in terms of components of specific discharge. The corresponding system of ordinary differential equations describing particle movement is:

$$\frac{dx}{dt} = \frac{u_{1,2}}{v_{1,2}}, \quad \frac{dy}{dt} = \frac{u_{1,2}}{v_{1,2}}$$

$$\begin{cases} u_1 = -\frac{Q}{2\pi} \left[\frac{C}{C^2+y^2} - \frac{\lambda R^2 A}{A^2+B^2} \right], & \begin{cases} u_2 = -\frac{Q(1-\lambda)}{2\pi} \frac{C}{C^2+y^2}, \\ v_2 = -\frac{Q(1-\lambda)}{2\pi} \frac{y}{C^2+y^2}, \end{cases} \\ v_1 = -\frac{Q}{2\pi} \left[\frac{D}{C^2+y^2} - \frac{\lambda R^2 B}{A^2+B^2} \right], \end{cases} \quad (5.1)$$

where

$A = R^2x - x_0(x^2 - y^2)$, $B = R^2y - 2x_0xy$, $C = x - x_0$, $\lambda = (k_1 - k_2)/(k_1 + k_2)$
 u_1, v_1 are specific discharge components for the aquifer and u_2, v_2 for the inclusion,
 $v_{1,2}$ are porosities of the two media.

We start with the particles placed along a circle of large radius ρ_1 surrounding the well and track them until a circle of small radius ρ_2 surrounding the active well. System (5.1) is integrated analogously to the previous cases. Fig. 13 shows isochrones (curves 1-7 correspond to $t = 0, 1.5, 3.0, 4.5, 6.0, 7.5, 9.0$) for $\rho_1/R = 4.0$, $Q/(kR) = 1.0$, $x_0/R = 2.1$, $v_1 = v_2 = 0.2$, and $k_2/k_1 = 0.2, 5.0$ (plots a-b, respectively). The significantly curved fronts for large times illustrate considerable deviation of the breakthrough curve from a simple 'step' valid for a homogeneous aquifer. Fig. 14 shows for the same $\rho_1, \rho_2, x_0, v_1, v_2, Q$ the distributions of travel times $\delta T = T - T^0$ as functions of θ/π where $T^0 = \pi v(\rho_1^2 - \rho_2^2)/Q$ is the travel time for a homogeneous aquifer. Curves 1-4 in Fig. 14 correspond to $k_2/k_1 = 0.2, 0.6, 1.8, 5.4$. This time difference characterizes advection of equidistantly placed particles toward the active well. From these graphs we infer that even a very simple circular inhomogeneity causes non-trivial changes in travel time distributions, to wit $T(\theta)$ exhibits a local maximum (retardation) and minimum (acceleration) for more and less conductive inclusions, respectively. In other words, the 'fastest' and 'slowest' streamlines are not straight ones. The graphs also show that the celerity of particle breakthrough is higher for one part of the starting circle (negative δT) and lower for another one

(positive δT) as compared with the case $k_1 = k_2$. We used a ρ_1 -circle surrounding the pumping well as position for starting points though these points can be selected arbitrary.

The results above can be interpreted for analysis of pumping when an aquifer under operation contains low-permeable lenses (Tiedeman 1995) which are a potential source of contamination because of previously sorbed species.

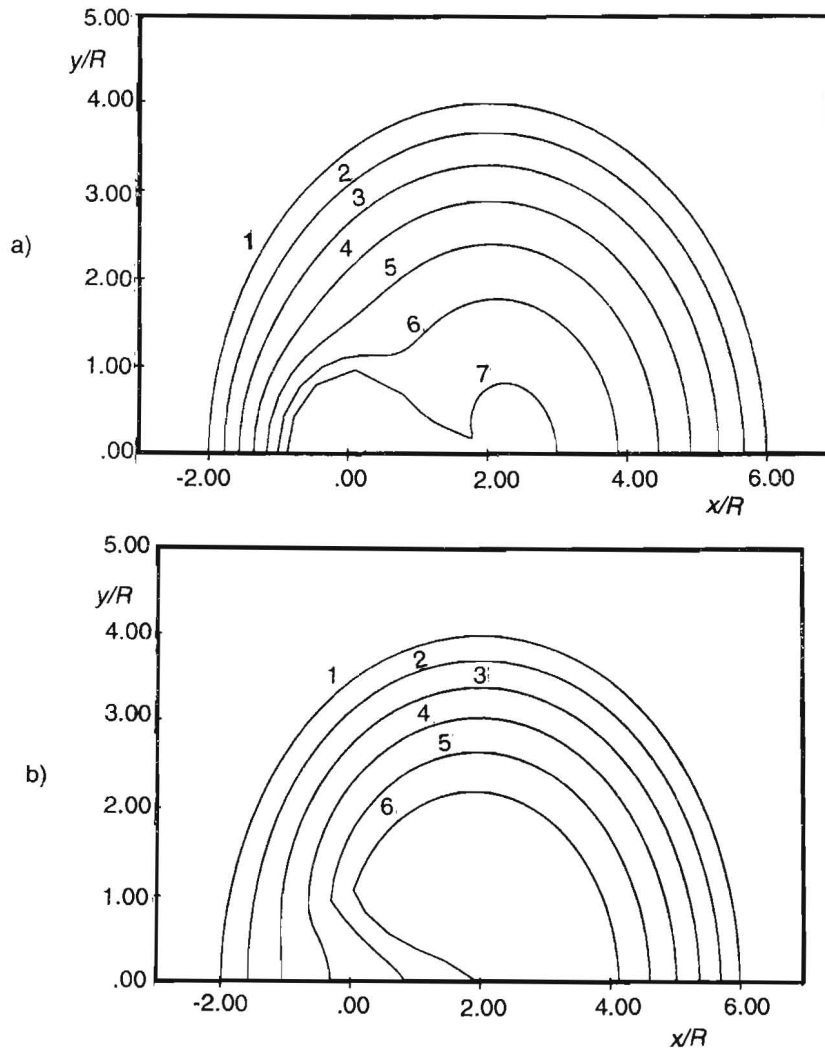


Fig. 13. Isochrones for a) less permeable, b) more permeable inclusions.

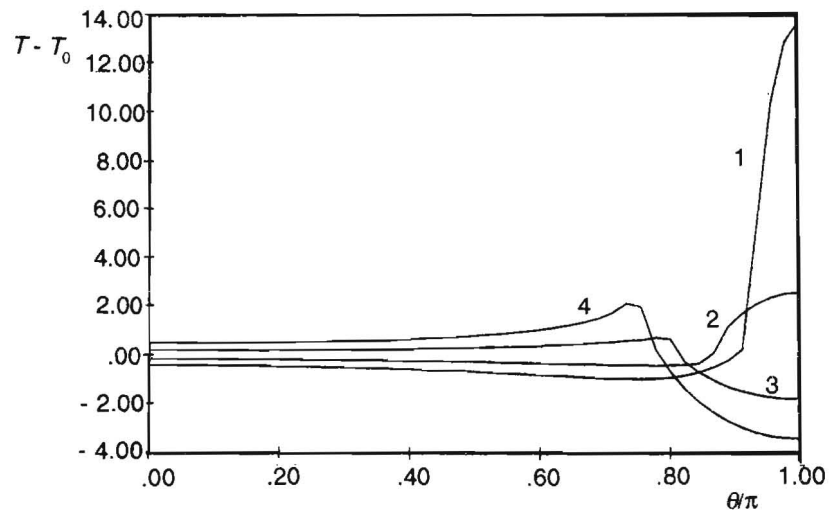


Fig. 14. Travel time distributions.

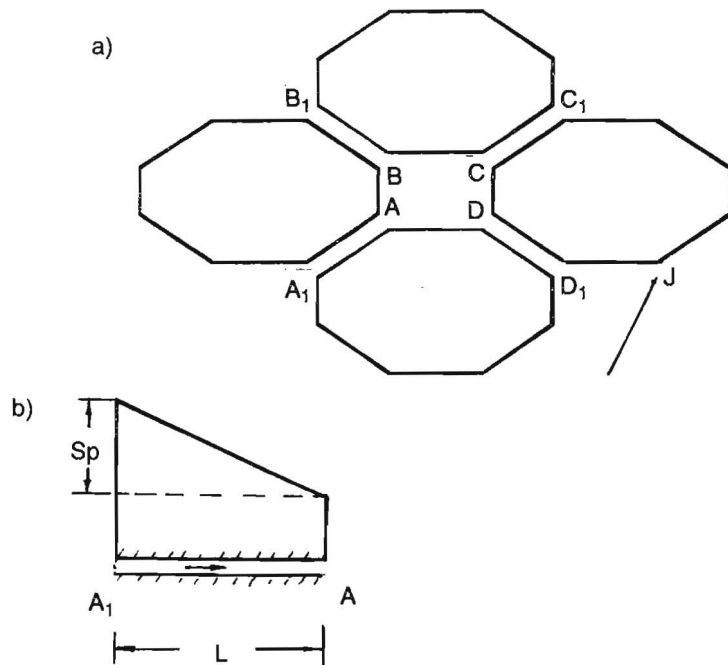


Fig. 15. Octagonal block structure: a) one element of the whole network, b) 1-D fracture element.

Conclusions

Explicit form of the velocity field like (2.3), (4.3), (4.4), (5.1) allows for evaluation of all flow characteristics with the error of numerical integration which can be estimated analytically and can be made arbitrary small by proper choice of the time step. Hence, they can serve as test procedures for the numerical methods used in widely spread software like MODFLOW or MT3D where the flow problem is solved in terms of head (pressure) and particle tracking involves numerical differentiation (Anderson and Woessner 1992).

We showed that Muskat's IEW flow patterns are limiting cases of a two-component double-periodic chekerboard system. The explicit solutions derived can serve as 'elements' of other network system. For example, return to the periodic case shown in Fig. 1a with $k_2 = 0$ and show how our solution can be interpreted as an element of a more complex structure. Namely, consider a network of impermeable octogonal blocks composed in such a way that this fractures intersect at nearly rectangular junctions (Fig. 15a). Both void space $ABCD$ and fractures AA_1 , BB_1 , CC_1 , DD_1 are filled with a porous material.

The corresponding Darcy flow can be decoupled into two elements: 2-D flow within junctions as studied above and 1-D flow within fractures. For the last one we use the well-known formula $q_a = kb\delta p/L$ where k is conductivity of the filling material, b is the fracture aperture, L is the fracture length. The pressure (head) loss δp along one fracture (Fig. 15b) can be matched with the head loss in the 2-D rectangular element $ABCD$ in an approximate way.

Noteworthy, that the results obtained can be utilized in mathematically equivalent problems involving point singularities (Buchholz 1957, Carslaw and Jaeger 1959) as well as many solutions from electrodynamics, thermophysics, diffusion theory can be easily reformulated in terms of subsurface flows.

Acknowledgments

This study was supported by USIA-CIES, grant N18967 and the Russian Foundation of Basic Research, grant N 96-01-123. Helpful comments made by two anonymous reviewers are highly appreciated.

References

- Abramowitz, M. and Stegun, I.A** (1970) *Handbook of Mathematical Functions*, Dover, New York.
- Anderson, M.P. and Woessner, W.W.** (1992) *Applied Groundwater Modeling: Simulation of Flow and Advective Transport*, Academic Press, San Diego.
- Arnold, V.I.** (1983) *Geometrical Methods in the Theory of Ordinary Differential Equations*, Springer-Verlag, New York.
- Buchholz, H.** (1957) *Elektrische und magnetische Potentialfelder*, Springer Verlag, Berlin.
- Carslaw, H.S. and Jaeger, J.C.** (1959) *Conduction of Heat in Solids*, Oxford University Press, London.
- Child, K.A.** (1985) In-ground barriers and hydraulic measures, in **Smith, M.A. (ed.)**, *Contaminated Land. Reclamation and Treatment*: 145-182 pp.
- Emets, Yu.P. and Obnosov, Yu. V.** (1989) Exact solution of the problem of current generation in a doubly periodic heterogeneous system, *Sov. Phys. Dokl.* **34**: 972-974.
- Emets, Yu.P. and Obnosov, Yu. V.** (1990) Compact analog of a heterogeneous system with a checkerboard field structure, *Sov. Phys. Tech. Phys.*, **35**: 907-913.
- Firoozabadi, A. and Markeset, T.** (1995) Laboratory studies in fractured porous media, P.II. Capillary crossflow, *In Situ*, **19**: 23-39.
- Ground Water Contamination and Methodology.** US Environmental Protection Agency, (1992) Technomic Publishing Co., Lancaster, Pa.
- Grove, D.B., Beteem W.A. and Sower, F.B.** (1970) Fluid travel time between a recharging and discharging well pair in an aquifer having a uniform regional flow field, *Water Resour. Res.*, **6**: 1404-1410.
- Kacimov, A.R. and Obnosov, Yu.V.** (1994) Minimization of ground water contamination by lining of a porous waste repository, *Proc. India Natl. Sci. Acad., P.A.*, **60**: 783-792.
- Kacimov, A.R. and Obnosov, Yu.V.** (1995) Ground water flow in a medium with periodic inclusions, *Izv. RAN, Mekhanika Zhidkosti i Gasa* **30**, N5: 139-148 (in Russian), Engl. transl.: *Fluid Dynamics*, 1995, **30**, N5.
- Kinzelbach, W.** (1992) *Numerische Methoden zur Modellierung des Transports von Schadstoffen im Grundwasser*, Oldenbourg Verlag, Munchen.
- Kung, K.J.S.** (1990) Preferential flow in a sandy vadoze zone, 1. Field observation, *Geoderma*, **46**: 51-58.
- Muskat, M.** (1946) *Physical Principles of Oil Production*, McGraw Hill, New York.
- Obnosov, Yu. V.** (1992) Solution of certain boundary problem of R-linear conjugation with piecewise-constant coefficients. *Russian Mathematics*, **36**(N4): 38-47.
- Obnosov, Yu. V.** (1996) Exact solution of a problem of R-linear conjugation for a rectangular checkerboard field. *Proc. Royal Soc. London, A* (in press).
- Petroleum Production Handbook. V.2. Reservoir Engineering.** (1962), McGraw Hill, New York.
- Philip, R.D. and Walter, G.R.** (1992) Prediction of flow and hydraulic head fields for vertical

circulation wells, *Ground Water*, **30**(N5): 765-773.

Polubarinova-Kochina, P.Ya. (1977) *Theory of Ground Water Movement*, Nauka, Moscow (in Russian).

Rankine, W.J.H. (1871) On the mathematical theory of stream-lines. especially those with four foci and upwards. *Philosophical Transactions*, **161**: 267-306.

Rowe, R.K. (1988) Eleventh Canadian geotechnical colloquium: contaminant migration through groundwater- the role of modelling in the design of barriers, *Can. Geotech. J.*, **25**: 778-798.

Strack, O.D.L. (1989) *Groundwater Mechanics*, Prentice Hall, Englewood Cliffs.

Tiedeman, C.R., Hsieh P.A. and Christian, S.B. (1995) Characterization of a high-transmissivity zone by well test analysis: steady state case, *Water Resour. Res.*, **31**: 25-37.

Wilson, J.L. (1984) Double-cell hydraulic containment of pollutant plumes, in *Proc. Fourth National Symposium on Aquifer Restoration and Ground Water Monitoring*, National Water Well Association, Dublin, Ohio: 65-70 pp.

(Received 23/09/1995;
in revised form 01/05/1996)

حلول تحليلية لمسألة تدفق المصب - المنبع في وسط مسامي

أنور قاسيموف و يوسف أوبنوسوف

معهد الرياضيات والميكانيكا - جامعة كازان الحكومية
١٧ شارع الجامعة - ٤٢٠٠٠٨ - كازان - تاتراستان - روسيا

تُعتبر النمذجة الرياضية لتدفق الموائع ونقل الكيماويات تحت سطح الأرض تحت تأثير أنظمة الحقن والاستخراج ذات أهمية كبيرة في كل من هندسة النفط وعلم الهيدرولوجيا . وتستخدم هذه الأنظمة في تقنية الغمر (مسكات ١٩٤٦ Muskat) والصراف (ستراك ١٩٨٩ Strack) وفي طرق ضخ ومعالجة الطبقات الحاملة الملوثة (الوكالة الأمريكية لحماية البيئة ١٩٩٢ USEPA) .

في الطريقة التقليدية فإن الحقن والاستخراج من الآبار يمثل بواسطة المنابع والمصببات . يفرض أن الطبقات الحاملة/ الخزانات متجانسة . هذا يسمح بالوصف التحليلي للضغط (الضاغط الهيدروليكي) والسرعة وأوقات تحرك الجزئيات . . . الخ (مسكات ١٩٤٦ Muskat بوليبارينوفا - كوشينا ١٩٧٧ Polubarinova-Kochinal) . تصف هذه الخصائص مركبة الحركة الأفقية للانتقال التلوثي (أندرسون و ووسنر ١٩٩٢ Anderson and Woessner) . ومع ذلك فإن أي خزان حقيقي أو طبقة حاملة هي ليست متجانسة ولا تُعرف سوى

حلول تحليلية قليلة حتى بالنسبة لأبسط النماذج (المائع الأحادي والطبقة الحاملة المحصورة والتوصيل الثابت متدرج التغير . . . الخ) . وفي تحليل رياضي جديد تم تطويره بواسطة (إميتس وأبنسوف ١٩٨٩ ، Amets ١٩٩٠ and Obnosov) .

توصل أبنسوف (١٩٩٢ Obnosov) لوصف صريح للحركة الأفقية للموائع مع ظروف انكسار شديدة على طول الحدود بين طبقات ذات نفاذيات مختلفة . ولقد استخدمت هذه الطريقة حديثاً في تطبيقات تدفق المياه الجوفية في الطبقات الحاملة (قاسيموف وأبنسوف ١٩٩٤ ، Kacimov and ١٩٩٥ Obnosov) .

في هذا البحث يقدم الباحثان وصفاً صريحاً قوياً لمشكلة التدفق في خزان يحتوي على تكوينات مستطيلة دورية مزدوجة من النوع العدسي . ونتيجة لذلك فإن التدفق الطبيعي يتحول إلى ثنائي الأبعاد ذي خطوط تدفق منحنية ويتحول النقل التلوثي إلى خطوط تدفق إصبعية أو قناتية . ولقد تم استخدام أبسط النماذج الخاصة بالتدفق الأفقي للموائع مع إهمال جميع الآليات الأخرى (الامتصاص الكتلي والتشتت الصغير . . . الخ) .

في بادئ الأمر تم بحث الحالة الحديثة عندما تكون الكتل غير منفذة . ويصف هذا الحل السرعة (التدفق النوعي) كدالة غير تحليلية داخل الخلية الابتدائية (المستطيلة) مع نقاط شاذة مصب - منبع عند رؤوسه . كحالة خاصة تم التوصل إلى أنظمة حقن - استخراج من الآبار ذات تماثل . وعليه فإن الشبكة الخطية والشبكة عشبية النوع وبالات الشبكة ذات النقاط الخمس جاءت من الحالة العامة عند معدلات متساوية من الحقن والاستخراج . وتم تقديم الحلول على شكل معادلات محكمة بدلالة الدوال الناقصية بالإضافة

لمفكوكات متسلسلات مسكات . وكنوع من اختبار طريقة تتبع الجزئيات المستخدمة تم حساب خطوط التدفق ، خطوط العزل والسرعات المتوسطة لاثنين من الأنظمة الهيدرولوجية . بالتحديد تم اعتبار زوج آبار الحقن - سحب ثنائي الأقطاب الكائن في تدفق مياه جوفي منتظم كجسم رانكين . هذا النظام يستخدم في تجارب التعقب وأنظمة الاستخراج والمعالجة لمعالجة الطبقات الحاملة . كما استخدم حل بوليبارينوفا-كوشينا التحليلي لحساب خصائص التدفق الأفقي للموائع المذكورة لحالة استخراج الماء من بئر محفور في طبقة تحتوي على عدم تجانس دائري . أخيراً تمت مناقشة تطبيقات النظام العدسي لشبكات نمذجة وسط متفتت ذي كتل عشرية .